

Fluorescence Lifetimes and Correlated Photon Statistics from Single CdSe/Oligo(phenylene vinylene) Composite Nanostructures

M. Y. Odoi,[†] N. I. Hammer,[†] K. T. Early,[†] K. D. McCarthy,[†] R. Tangirala,[‡]
T. Emrick,[‡] and M. D. Barnes^{*,†}

*George R. Richason, Jr. Chemistry Research Laboratory, Department of Chemistry
and Department of Polymer Science and Engineering, University of Massachusetts,
Amherst, Massachusetts 01003*

Received June 1, 2007; Revised Manuscript Received July 16, 2007

ABSTRACT

We present measurements of fluorescence intensity trajectories and associated excited-state decay times from individual CdSe/oligo(phenylene vinylene) (CdSe–OPV) quantum dot nanostructures using time-tagged, time-resolved (TTTR) photon counting techniques. We find that fluorescence decay times for the quantum dot emitter in these composite systems are at least an order of magnitude shorter than ZnS-capped CdSe quantum dot systems. We show that both the blinking suppression and associated lifetime/count rate behavior can be described by a modified version of the diffusive reaction coordinate model which couples slow fluctuations in quantum dot electron ($1S_e$, $1P_e$) energies to Auger-assisted hole trapping processes, hence modifying both blinking statistics and excited-state decay rates.

Fluorescence intermittency (“blinking”)^{1–9} is both a troublesome and fascinating aspect of semiconductor quantum dot (QD) luminescence in solid-state systems.^{6,7,10–19} Blinking—which can occur on time scales of tens of seconds—is especially problematic for quantum dot based optoelectronic devices or applications involving molecular tracking in biological systems.^{8,20–23} As a result, the mechanism of QD blinking, and blinking suppression, has attracted a great deal of theoretical interest.^{2,9,22,24,25} In addition, several recent experimental reports of blinking suppression in QD systems have pointed to conducting surfaces or electron-donating species at the QD surface as playing a critical role in this modified photophysical behavior.^{5,26} These electron donating species are thought to render trap sites on the nanocrystal surface unavailable for the formation of a charge separated state, so a radiative recombination pathway for exciton decay becomes dominant. In our own recent work, we showed that CdSe QDs, whose surfaces were derivatized with conjugated organic ligands, displayed a high degree of blinking suppression that was attributed, in part, to electron transfer to the QD surface from photoexcited ligands. In this Letter, we describe time-tagged, time-resolved (TTTR) measurements on CdSe/oligo(phenylene vinylene) (CdSe–OPV)

nanostructures that exhibit suppressed blinking in the solid state. We show that the luminescence intensity as a function of time is weakly correlated with excited-state lifetime. Interpretation of this result within the diffusive coordinate model suggests that a modified Auger-assisted hole-trapping rate (provided by the surface ligands) can account for the observed photon statistics and lifetime behavior.

Functionalization of QDs with complex ligands promises not only to create hybrid nanostructures with interesting energy and charge-transfer properties but also to help elucidate the role that the surface “environment” plays in modulating the quantum confined core and surface states involved in radiative or nonradiative transitions. Explanations of many phenomena in QDs such as spectral diffusion²⁷ and photodarkening recovery²⁸ based on surface effects have been ubiquitous in the literature. Recently, Frantsuzov and Marcus⁹ have proposed a diffusive coordinate (DC) model describing the blinking behavior as a result of surface hole-trapping processes which depend on the instantaneous difference, ϵ , between the ($1S_e$, $1P_e$) QD electron energy levels.² In our previous work, we observed an average dark state dwell time of 500 ms for individual CdSe QDs derivatized with phenylene vinylene oligomers, compared to ZnS-capped CdSe QD systems that showed an average dark-state dwell time of tens of seconds.^{29–31} However, since the time resolution of these previous experiments was limited by the

* Author to whom correspondence should be addressed.

[†] Department of Chemistry.

[‡] Department of Polymer Science and Engineering.

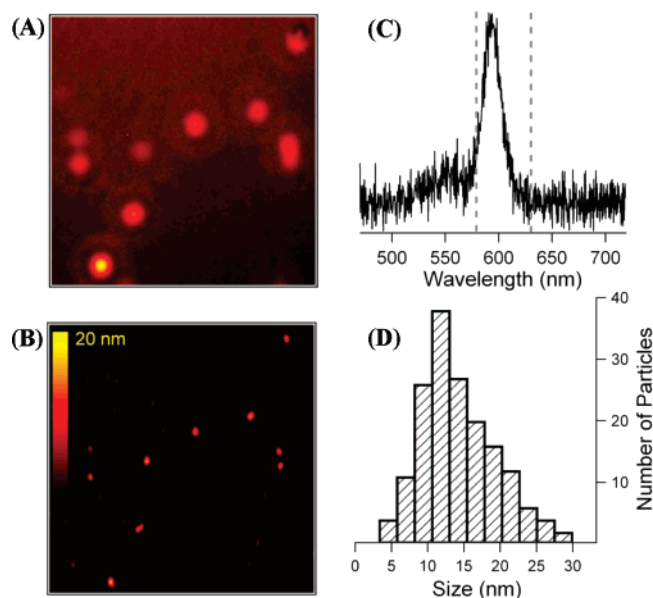


Figure 1. Spatially registered fluorescence (A) and AFM (B) images of the same scene of individual CdSe-OPV nanostructures. Shown in (C) is a representative spectrum from an individual CdSe-OPV nanostructure with the dotted gray lines indicating the spectral window of the bandpass filter employed for the photon counting experiments. Panel D shows a histogram summarizing the height measurements for 92 individual CdSe-OPV nanostructures.

CCD camera data rate to ≥ 100 ms, no information on finer time scales or associated fluorescence decay rate—a critical piece of information in the DC model—was available.

Here, we present experimental results on the excited-state decay dynamics and associated photon statistics of individual CdSe-OPV composite nanostructures using time-tagged, time-resolved (TTTR) single photon counting techniques. TTTR allows access both to the arrival time of emitted photons relative to the excitation pulse and to the time stamp of the detected photon relative to the start of data acquisition. From this photon-by-photon analysis,³² both intensity and lifetime trajectories can be constructed and can show the correlation between decay rates and intensity. Recently, Yang and co-workers have used this technique to measure fluorescence intensity trajectories from isolated ZnS-capped CdSe QDs and observed a distribution of “gray” intensity levels correlated with different fluorescence lifetimes.^{33,34}

Samples of CdSe-OPV and ZnS-capped CdSe QDs with core diameters of ~ 4.3 nm were prepared by reported methods.³⁵ Individual CdSe/ZnS QDs or CdSe-OPV nanostructures were isolated from ultradilute ($\sim 10^{-10}$ M) solutions in tetrahydrofuran (Fisher Scientific Optima grade) on plasma-cleaned glass cover slips. Fluorescence measurements were performed on a Nikon Eclipse-TE2000U inverted microscope with 1.4NA 100 \times oil objective in a total internal reflection (TIR) configuration. A Digital Instrument Bioscope (BS3-N, tapping mode) mounted on the TE300 microscope, was used for atomic force microscope (AFM) imaging.^{29,30} TTTR data were acquired using a 440 nm pulsed diode laser (PDL-800-LDH-C440, Picoquant, GmbH) as an excitation source, with a repetition rate of 10 MHz and pulse width of 50 ps full width at half-maximum. The total average power

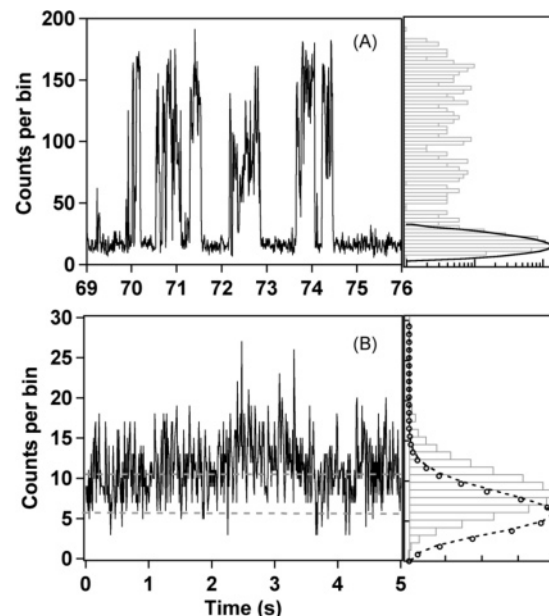


Figure 2. Representative intensity trajectories from a single CdSe/ZnS quantum dot (A) and individual CdSe-OPV nanostructure (B) obtained in TTTR mode, with a 10 ms time bin. On the right (gray) are count distributions of each time trace superimposed with each background count distribution (solid black for CdSe/ZnS and dashed black for CdSe-OPV). The circles in B represent a Poisson fit to the background distribution with a mean of 6.5 counts.

at the sample was 200 μ W in a defocused spot of about 15 μ m diameter and was the same for both ZnS-capped CdSe and CdSe-OPV samples. The fluorescence was filtered through a 605/50 nm band-pass filter, centered approximately at the peak emission wavelength of the QDs used in these experiments. A Perkin-Elmer Optoelectronics, SPCM-AQR-14 avalanche photodiode (APD) was used for photon counting, and a TimeHarp 200 (Picoquant GmHB) time-to-digital converter PCI board was used for generating the TTTR data record. All TTTR data on individual nanostructures were acquired for 300 s. Comparisons of count rates under similar excitation and detection with ref 16 indicate that we are well within a linear excitation regime. Fluorescence decay rates within various time/intensity segments of the trajectory were obtained by either least-squares fitting or a maximum likelihood estimate (MLE) algorithm.^{36–38}

Figure 1A shows a typical fluorescence image of several individual CdSe-OPV nanostructures obtained using a CCD camera registered with an AFM height scan (Figure 1B). The height histogram of the CdSe-OPV sample (Figure 1D) is peaked at ~ 12 nm, consistent with a 4.3 nm CdSe core fully coordinated with OPV ligands with average lengths of ~ 4.5 nm.²⁹ Figure 1C shows a typical emission spectrum from a single CdSe-OPV nanostructure indicating that essentially all the fluorescence intensity is associated with CdSe luminescence with a negligible contribution from the OPV.³⁰ Also indicated on Figure 1C are the blue- and red-transmission edges of the band-pass filter (vertical dashed lines) used in the TTTR experiments which further ensure that OPV emission does not contribute to the measured APD signals.

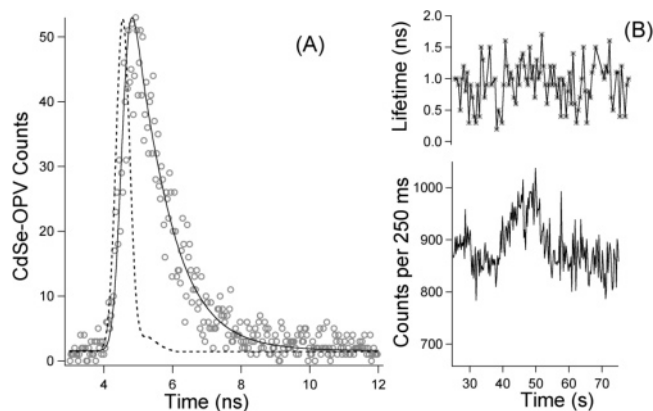


Figure 3. (A) Typical fluorescence decay curves from an individual CdSe-OPV nanostructure (open circles), with instrument response function (dashed line) and convolved fit to a single-exponential decay (solid line). The full width half-maximum of the instrument response function was 550 ps, and the value for τ extracted from the fit was 0.850 ± 0.040 ns. (B) Fluorescence lifetime and corresponding intensity trajectories from an individual CdSe-OPV nanostructure (top and bottom panels, respectively).

Figure 2 shows a comparison of intensity trajectories of an individual ZnS-capped CdSe QD and a CdSe-OPV nanostructure from TTTR measurements using a 10 ms time bin. In the case of CdSe/ZnS QD shown in Figure 2A, the fluorescence emission displays varying levels of intensity in qualitative agreement with the results reported by Yang and co-workers.³⁴ The photocount distribution (probability of measuring N photons as a function of N) is displayed to the right of each intensity trajectory; for CdSe/ZnS, this distribution is dominated by background indicating that the particle spends a significant fraction of the total trajectory in the dark state. Figure 2B shows an intensity trajectory and a corresponding photocount histogram from a typical CdSe-OPV nanostructure. Superimposed on the fluores-

cence photocount distribution is a histogram of background (source noise and APD dark counts) distribution characterized by a Poisson distribution with mean value 6.5. Fitting our measured photocount distribution from a single CdSe-OPV particle as a sum of background and signal (Poisson) distributions indicates a background contribution to the data of about 18%. Even at 10 ms time resolution, we find little evidence of extended dark-state dwell times. Using a 3σ threshold to discriminate between “bright” and “dark” states, we find an exponential distribution of dark-state dwell times with a $1/e$ dwell-time value of 170 ms. This value is in reasonable agreement with the $\langle\tau_{\text{off}}\rangle$ estimate of 500 ms obtained previously from CCD measurements.²⁹

Correlations between the fluorescence decay rate and count rate, accessed directly from the TTTR data record, provide important insights into the exciton dynamics of the particles. Measurements on ZnS-capped CdSe nanoparticles (not shown) exhibit fluorescence decay times between 20 and 28 ns, with a positive correlation between intensity and decay time consistent with results reported Yang and others^{4,33,34} and the model of Verberk et al.^{2,39} Analysis of decay times from individual CdSe-OPV nanostructures, shown in Figure 3A, reveals significantly shorter decay times (0.850 ± 0.040 ns). The fluorescence intensity trajectories with associated lifetime trajectories for CdSe-OPV (Figure 3B) suggest a weak positive correlation between intensity and fluorescence lifetimes (ranging from 500 ps to 2.5 ns); however the relatively long binning times imposed by signal-to-noise constraints may obscure larger-scale fluctuations. For the time period 25–40 s, the integrated signal was 860 counts with an average lifetime of 0.8 ns, whereas during the intensity burst (40–55 s) the integrated signal was 932 counts with an average lifetime of 1.1 ns.

The similar correlation between excited-state lifetime and fluorescence intensity (count rate) between the ZnS-capped

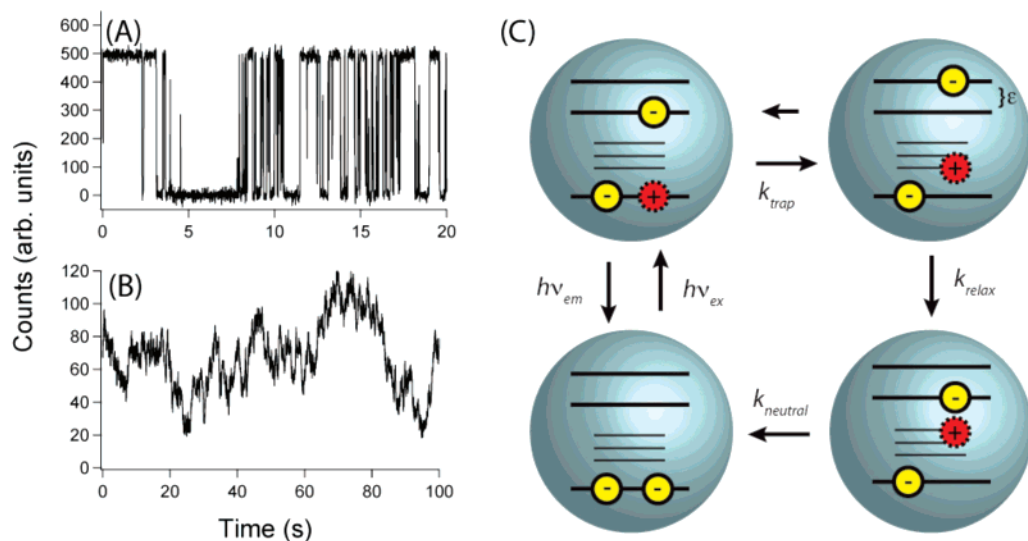


Figure 4. Simulation results for the diffusive coordinate (DC) model. (A) A narrow (Gaussian) line shape function for trap states results in intensity traces similar to the fluorescence observed in CdSe/ZnS dots, namely a binary, blinking intermittency. (B) A broader (Lorentzian) line shape function for trap states with an altered value for both the center and width of the diffusive motion yields results similar to the fluorescence observed in CdSe-OPV nanostructures. (C) Simplified state diagram describing exciton radiative vs nonradiative recombination in CdSe-based quantum dot systems.

and OPV-covered dot systems provides compelling evidence for a common mechanistic origin. In the diffusive coordinate model proposed by Frantuzov and Marcus, QD blinking derives from a light-induced diffusional “motion” of the energy separation between the first two quantum dot electron states ($\epsilon = E_{\text{ISE}} - E_{\text{IPE}}$) and the effect of these fluctuations on the nonradiative recombination rate initiated by hole trapping on the nanocrystal surface.⁹

Figure 4 shows the results of kinetic simulations using the DC model, along with a simplified state diagram that describes radiative versus nonradiative recombination of excitons in CdSe-based quantum dot systems, where k_{nr} (determined by the rates for individual steps k_{trap} , k_{relax} , and k_{neutral}) represents the primary nonradiative recombination pathway. The results of two slightly different models are presented: in the first, a narrow (Gaussian) form for the surface trap state lineshapes results in a “binary” on/off, or blinking behavior, due to a hard boundary between regions (in ϵ space) of dominant/suppressed nonradiative transitions. In regions of ϵ space where nonradiative decay dominates over radiative decay, no fluorescence is observed. This behavior resembles the intensity trajectories observed in single CdSe/ZnS QDs. In the second model, numerical simulation shows blinking suppression and intensity fluctuations that result when a broader (Lorentzian) line shape is assumed for the surface trap states, precisely the type of behavior observed in our CdSe–OPV composite system. These numerical results suggest that our modified DC model characterizes a line broadening of the surface traps due to the presence of OPV ligands resulting in modified nonradiative dynamics of the system. A recent experiment⁴⁰ probing the effect of substrate on blinking statistics shows fluorescence time traces of CdSe/ZnS dots on indium tin oxide that bear a striking resemblance to the time traces of CdSe–OPV nanostructures, featuring both blinking suppression and intensity fluctuations described for our CdSe–OPV nanostructures. The similarities in these results point to the importance of the electronic environment surrounding the dot and lead us to speculate that these nearby electronic degrees of freedom are the environment which has the most direct effect on the surface hole-trapping physics responsible for modulating the photoluminescence.

In conclusion, we have shown that the fluorescence properties of individual hybrid CdSe–OPV nanostructures are strikingly different from conventional ZnS-capped CdSe QDs. Fluorescence-correlated AFM measurements show that the size distribution of these nanostructures is consistent with earlier results, with the most probable size ~ 12 nm. Time-tagged, time-resolved single photon counting measurements reveal a very short fluorescence lifetime for the CdSe–OPV composite systems compared to the CdSe/ZnS. The fluorescence decay times of the CdSe–OPV are correlated with intensity but, surprisingly are contained within a very narrow distribution. We suggest that the OPV ligands form a strongly coupled electronic bath that forms the environment controlling energetic fluctuations, and hence nonradiative trapping kinetics in the CdSe quantum dot.

Acknowledgment. We acknowledge the support of the NSF-Sponsored Center of Hierarchical Manufacturing at UMass–Amherst (DMI-0531171), NSF-Sponsored MRSEC at UMass–Amherst, US-DOE Basic Energy Sciences (05ER15695), and the Intelligence Community Postdoctoral Fellowship Program.

References

- (1) Zwiller, V.; Blom, H.; Jonsson, P.; Panev, N.; Jeppesen, S.; Tsegaye, T.; Goobar, E.; Pistol, M. E.; Samuelson, L.; Bjork, G. *Appl. Phys. Lett.* **2001**, *78*, 2476–2478.
- (2) Verberk, R.; van Oijen, A. M.; Orrit, M. *Phys. Rev. B* **2002**, *66*, 233202.
- (3) Shimizu, K. T.; Neuhauser, R. G.; Leatherdale, C. A.; Empedocles, S. A.; Woo, W. K.; Bawendi, M. G. *Phys. Rev. B* **2001**, *63*, 205316.
- (4) Schlegel, G.; Bohnenberger, J.; Potapova, I.; Mews, A. *Phys. Rev. Lett.* **2002**, *88*, 137401.
- (5) Ray, K.; Badugu, R.; Lakowicz, J. R. *J. Am. Chem. Soc.* **2006**, *128*, 8998.
- (6) Nirmal, M.; Dabbousi, B. O.; Bawendi, M. G.; Macklin, J. J.; Trautman, J. K.; Harris, T. D.; Brus, L. E. *Nature* **1996**, *383*, 802–804.
- (7) Lounis, B.; Bechtel, H. A.; Gerion, D.; Alivisatos, P.; Moerner, W. E. *Chem. Phys. Lett.* **2000**, *329*, 399–404.
- (8) Kuno, M.; Fromm, D. P.; Hamann, H. F.; Gallagher, A.; Nesbitt, D. J. *J. Chem. Phys.* **2000**, *112*, 3117–3120.
- (9) Frantsuzov, P. A.; Marcus, R. A. *Phys. Rev. B* **2005**, *72*, 155321.
- (10) Wang, X. Y.; Qu, L. H.; Zhang, J. Y.; Peng, X. G.; Xiao, M. *Nano Lett.* **2003**, *3*, 1103–1106.
- (11) Rossetti, R.; Ellison, J. L.; Gibson, J. M.; Brus, L. E. *J. Chem. Phys.* **1984**, *80*, 4464–4469.
- (12) Norris, D. J.; Efros, A. L.; Rosen, M.; Bawendi, M. G. *Phys. Rev. B* **1996**, *53*, 16347–16354.
- (13) Colvin, V. L.; Schlamp, M. C.; Alivisatos, P. A. *Nature* **1994**, *370*, 354.
- (14) Huynh, W. U.; Dittmer, J. J.; Alivisatos, P. A. *Science* **2002**, *295*, 2425.
- (15) Liu, J.; Tanaka, T.; Sivula, K.; Alivisatos, P. A.; Frechet, M. J. J. *Am. Chem. Soc.* **2004**, *126*, 6550–6551.
- (16) Gur, I.; Fromer, N. A.; Geier, M. L.; Alivisatos, P. A. *Science* **2005**, *310*, 462.
- (17) Fu, A. H.; Gu, W. W.; Larabell, C.; Alivisatos, A. P. *Curr. Opin. Neurobiol.* **2005**, *15*, 568–575.
- (18) Greenham, N. C.; Peng, X. G.; Alivisatos, A. P. *Phys. Rev. B* **1996**, *54*, 17628–17637.
- (19) Greenham, N. C.; Peng, X. G.; Alivisatos, A. P. *Synth. Met.* **1997**, *84*, 545–546.
- (20) Alivisatos, A. P.; Gu, W. W.; Larabell, C. *Annu. Rev. Biomed. Eng.* **2005**, *7*, 55–76.
- (21) Chan, W. C. W.; Nie, S. M. *Science* **1998**, *281*, 2016–2018.
- (22) Kuno, M.; Fromm, D. P.; Johnson, S. T.; Gallagher, A.; Nesbitt, D. J. *Phys. Rev. B* **2003**, *67*, 125304.
- (23) Kraus, R. M.; Lagoudakis, P. G.; Muller, J.; Rogach, A. L.; Lupton, J. M.; Feldmann, J.; Talapin, D. V.; Weller, H. *J. Phys. Chem. B* **2005**, *109*, 18214–18217.
- (24) Wang, L.; Califano, M.; Zunger, A.; Franceschetti, A. *Phys. Rev. Lett.* **2002**, *91*, 056404.
- (25) Marcus, R. A.; Tang, J. J. *J. Chem. Phys.* **2005**, *123*, 054704.
- (26) Hohng, S.; Ha, T. *J. Am. Chem. Soc.* **2004**, *126*, 1324–1325.
- (27) Blanton, S. A.; Hines, M. A.; Guyot-Sionnest, P. *Appl. Phys. Lett.* **1996**, *69*, 3905–3907.
- (28) Hess, B. C.; Okhrimenko, I. G.; Davis, R. C.; Stevens, B. C.; Schulzke, Q. A.; Wright, K. C.; Bass, C. D.; Evans, C. D.; Summers, S. L. *Phys. Rev. Lett.* **2001**, *86*, 3132–3135.
- (29) Hammer, N. I.; Early, K. T.; Sill, K.; Odoi, M. Y.; Emrick, T.; Barnes, M. D. *J. Phys. Chem. B* **2006**, *110*, 14167–14171.
- (30) Odoi, M. Y.; Hammer, N. I.; Sill, K.; Emrick, T.; Barnes, M. D. *J. Am. Chem. Soc.* **2006**, *128*, 3506–3507.
- (31) Hammer, N. I.; Emrick, T.; Barnes, M. D. *Nano. Res. Lett.* **2007**, *2*, 282–290.
- (32) Yang, H.; Xie, S. *J. Chem. Phys.* **2002**, *117*, 10965–10979.

- (33) Fisher, B. R.; Eisler, H. J.; Stott, N. E.; Bawendi, M. G. *J. Phys. Chem. B* **2004**, *108*, 143–148.
- (34) Zhang, K.; Chang, H.; Fu, A.; Alivisatos, A. P.; Yang, H. *Nano Lett.* **2006**, *6*, 843–847.
- (35) Skaff, H.; Sill, K.; Emrick, T. *J. Am. Chem. Soc.* **2004**, *126*, 11322–11325.
- (36) Edel, J. B.; Eid, S. J.; Meller, A. *J. Phys. Chem. B* **2006**, *111*, 2986–2990.
- (37) Kollner, M.; Fischer, A.; Arden-Jacob, A.; Drexhage, K.-H.; Muller, R.; Seeger, S.; Wolfrum, J. *Chem. Phys. Lett.* **1996**, *250*, 355–360.
- (38) Kollner, M.; Wolfrum, J. *Chem. Phys. Lett.* **2001**, *200*, 199–204.
- (39) Verberk, R.; Orrit, M. *J. Chem. Phys.* **2003**, *119*, 2214–2222.
- (40) Verberk, R.; Chon, J. W. M.; Gu, M.; Orrit, M. *Physica E* **2005**, *26*, 19–23.

NL0713068